Journal of Pharmacology and Toxicology

ISSN 1816-496X

Academic Journals Inc.

www.academicjournals.com

Journal of Pharmacology and Toxicology 2 (6): 567-573, 2007
ISSN 1816-496X

A Molecular Modelling Analysis of Luliconazole, Lanconazole and Bifonazole

Fazlul Huq
Discipline of Biomedical Science, School of Medical Sciences, Faculty of Medicine, Cumberland Campus, C42, The University of Sydney, Lidcombe, NSW, Australia

Abstract: In this study, molecular modelling analyses based on molecular mechanics, semi-empirical (PM3) and DFT (at B3LYP/6-31G* level) calculations have been carried out to obtain insight into their toxicity. The results of the analyses show that LLZ, LCZ and BFZ have LUMO-HOMO energy differences ranging from 4.5 to 4.9 eV, indicating that the compounds would be moderately inert with BFZ being the most inert one. The molecular surfaces of all the compounds are found to possess significant amounts of positively charged electron-deficient regions so that they may be subject to nucleophilic attacks by glutathione and nucleobases in DNA, thus causing cellular toxicity due to glutathione depletion and DNA damage due to oxidation of nucleobases. However, because of kinetic inertness of the molecules, the rates of such adverse reactions are expected to be low.

Key words: Luliconazole, lanconazole, bifonazole, antifungal agents, molecular modelling

INTRODUCTION

Luliconazole (LLZ), lanoconazole (LCZ) and bifonazole (BFZ) are optically active azole derivatives developed for use as antifungal agents in medicine and agriculture. They inhibit sterol 14α-methylase in fungal cells (Henry and Sisler, 1984). LLZ is an optically compound that exists in two enantiomeric forms: (-)-(E)-[(4R)-4-(2,4-dichlorophenyl)-1,3-dithiolan-2-ylidene] (1H-imidazol-1-yl) acetonitrile (R-LLZ) and (+)-(E)-[(4S)-4-(2,4-dichlorophenyl)-1,3-dithiolan-2-ylidene] (1H-imidazol-1-yl) acetonitrile (S-LLZ). LCZ and BFZ are also optically active existing in enantiomeric forms: (R)-lanoconazole (R-LCZ) and (S)-lanoconazole (S-LCZ), R-bifonazole (R-BFZ) and L-bifonazole (L-BFZ), respectively.

R-LLZ possesses a wide spectrum of antifungal activity and is very potent against dermatophytes, both *in vitro* and *in vivo* (Uchida *et al*., 2004; Koga *et al*., 2006). It is 2.5 and 28 times more effective in inhibition of ergosterol biosynthesis than racemic LCZ and R-BFZ respectively (Niwano *et al*., 1999). (S)-LLZ is almost inactive as an inhibitor 14α-demethylase, indicating that the stereochemical orientation of the 2,4-dichlorophenyl group plays an important role in interaction with the enzyme. On the contrary, both R-LCZ and S-LCZ are found to be active so that racemic LCZ can be used in therapy.

In this study, molecular modelling analyses have been carried out using the program Spartan '02 (Spartan, 2002) to investigate the kinetic lability of R-LLZ, S-LLZ, R-LCZ, S-LCZ, R-BFZ and S-BFZ and ease of their reaction with cellular nucleophiles, with the aim of providing a better understanding of their toxicity. The research was carried out in the Discipline of Biomedical Science, School of Medical Sciences, The University of Sydney during January to February 2007.

COMPUTATIONAL METHODS

The geometries of R-LLZ, S-LLZ, R-LCZ, S-LCZ, R-BFZ and S-BFZ have been optimised based on molecular mechanics, semi-empirical and DFT (Density functional theory) calculations, using the

molecular modelling program Spartan '02. Molecular mechanics calculations were carried out using MMFF force field. Semi-empirical calculations were carried out using the routine PM3. DFT calculations were carried at B3LYP/6-31G* level. In optimization calculations, a RMS gradient of 0.001 was set as the terminating condition. For the optimised structures, single point calculations were carried out to give heat of formation, enthalpy, entropy, free energy, dipole moment, solvation energy, energies for HOMO (highest occupied molecular orbotal) and LUMO (lowest unoccupied molecular orbital). The order of calculations: molecular mechanics followed by semi-empirical followed by DFT ensured that the structure was not embedded in a local minimum. To further check whether the global minimum was reached, some calculations were carried out with improvable structures. It was found that when the stated order was followed, structure corresponding to the global minimum or close to that could ultimately be reached in all cases. Although RMS gradient of 0.001 may not be sufficiently low for vibrational analysis, it is believed to be sufficient for calculations associated with electronic energy levels.

RESULTS AND DISCUSSION

Table 1 gives the total energy, heat of formation as per PM3 calculation, enthalpy, entropy, free energy, surface area, volume, dipole moment and energies of HOMO and LUMO as per both PM3 and DFT calculations for R-LLZ, S-LLZ, R-LCZ, S-LCZ, R-BFZ and S-BFZ. Figure 1-6 give the regions of negative electrostatic potential (greyish-white envelopes) in (a), HOMOs (where red indicates HOMOs with high electron density) in (b), LUMOs in (c) and density of electrostatic potential on

Table 1: Calculated thermodynamic and other parameters of R-LLZ, S-LLZ, R-LCZ, S-LCZ and BFZ

Molecule	Calculation type	Total energy (kcal mol^{-1}/ atomic unit*)	Heat of formation (kcal mol^{-1} K^{-1})	Enthalpy (kcal mol^{-1} K^{-1})	Entropy (kcal mol^{-1} K^{-1})	Free energy (cal mol^{-1} K^{-1})
R-LLZ	PM3	115.66	125.71	137.73	148.18	93.55
	DFT	-2419.88		138.97	147.45	95.03
S-LLZ	PM3	117.65	127.00	137.89	147.71	93.85
	DFT	-2419.88		138.99	147.13	95.14
S-LCZ	PM3	120.62	130.16	142.75	142.14	100.38
	DFT	-1960.29		143.38	141.79	101.13
S-LCZ	PM3	120.48	129.99	142.87	142.29	100.45
	DFT	-1960.25		143.44	141.75	101.20
R-BFZ	PM3	103.68	112.34	224.03	144.78	180.86
	DFT	-958.68		224.86	144.06	181.93
S-BFZ	PM3	103.69	112.49	224.21	143.81	181.38
	DFT	-958.68		224..87	143.15	182.21

Molecule	Calculation type	Solvation energy (kcal mol^{-1})	Area ($Å^2$)	Volume ($Å^3$)	Dipole moment (debye)	HOMO (eV)	LUMO (eV)	LUMO-MOMO (eV)
R-LLZ	PM3	-10.05	314.15	299.80	5.7	-9.01	-1.37	7.64
	DFT	-9.78	322.13	302.14	8.0	-6.30	-1.76	4.54
S-LLZ	PM3	-9.35	311.58	299.42	6.4	-8.97	-1.33	7.64
	DFT	-9.13	321.19	302.10	9.7	-6.20	-1.76	4.44
R-LCZ	PM3	-9.54	300.59	286.84	5.5	-9.01	-1.39	7.62
	DFT	-9.26	305.65	288.25	7.6	-6.23	-1.75	4.48
S-LCZ	PM3	-9.50	300.63	286.79	5.9	-9.00	-1.36	7.64
	DFT	-9.32	308.01	288.48	8.1	-6.23	-1.71	4.52
R-BFZ	PM3	-8.66	351.21	345.22	4.5	-9.29	-0.48	8.81
	DFT	-8.48	352.27	345.25	4.1	-5.93	-0.95	4.98
S-BFZ	PM3	-9.15	350.24	344.96	4.7	-9.38	-0.49	8.89
	DFT	-9.03	352.01	345.26	4.2	-5.94	1.04	4.90*

*In atomic units from DFT calculations

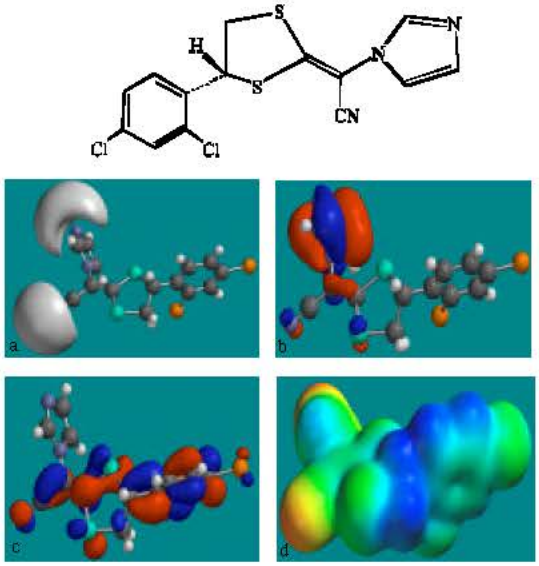

Fig. 1: Structure of R-LLZ giving in: (a) the electrostatic potential (greyish envelope denotes negative electrostatic potential), (b) the HOMOs, (where red indicates HOMOs with high electron density) (c) the LUMOs (where blue indicates LUMOs) and in (d) density of electrostatic potential on the molecular surface (where red indicates negative, blue indicates positive and green indicates neutral)

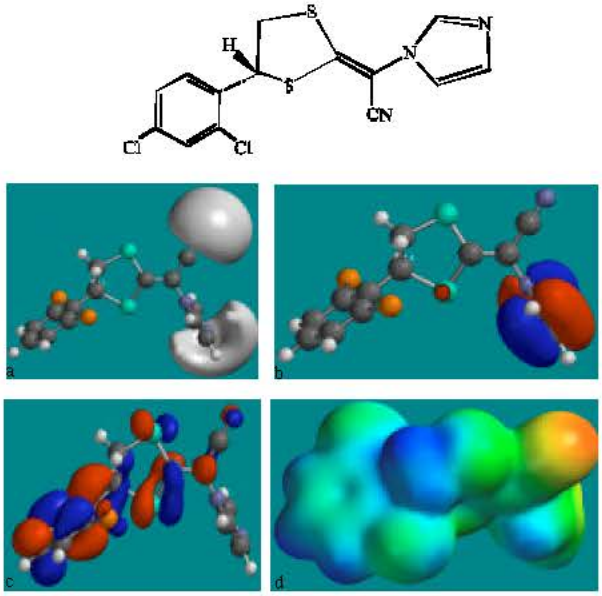

Fig. 2: Structure of S-LLZ giving in: (a) the electrostatic potential (greyish envelope denotes negative electrostatic potential), (b) the HOMOs, (where red indicates HOMOs with high electron density) (c) the LUMOs (where blue indicates LUMOs) and in (d) density of electrostatic potential on the molecular surface (where red indicates negative, blue indicates positive and green indicates neutral)

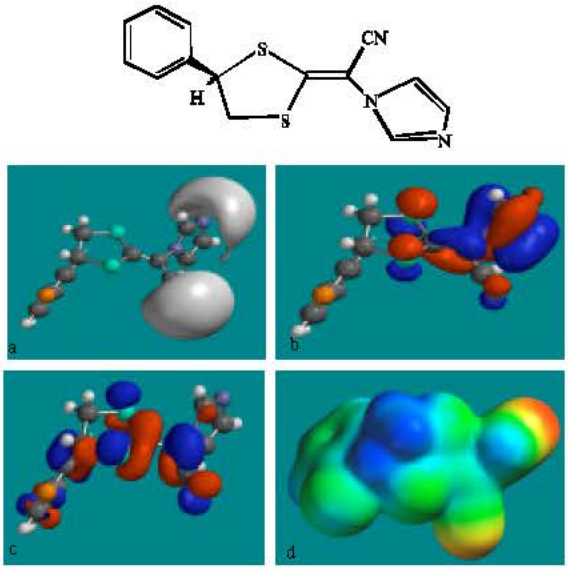

Fig. 3: Structure of R-RCZ giving in: (a) the electrostatic potential (greyish envelope denotes negative electrostatic potential), (b) the HOMOs, (where red indicates HOMOs with high electron density) (c) the LUMOs (where blue indicates LUMOs) and in (d) density of electrostatic potential on the molecular surface (where red indicates negative, blue indicates positive and green indicates neutral)

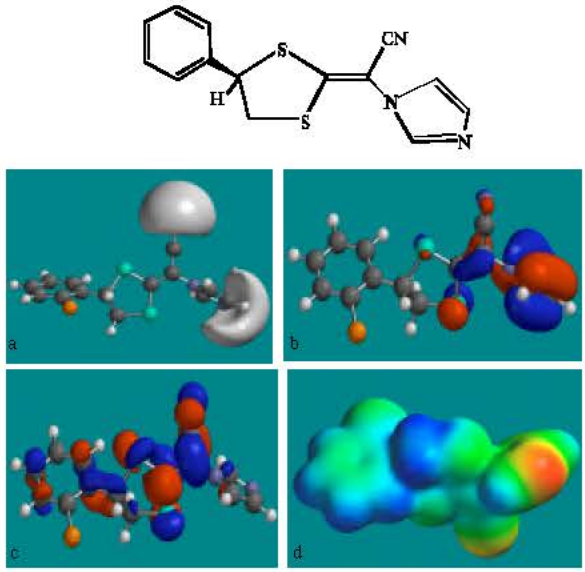

Fig. 4: Structure of S-RCZ giving in: (a) the electrostatic potential (greyish envelope denotes negative electrostatic potential), (b) the HOMOs, (where red indicates HOMOs with high electron density) (c) the LUMOs (where blue indicates LUMOs) and in (d) density of electrostatic potential on the molecular surface (where red indicates negative, blue indicates positive and green indicates neutral)

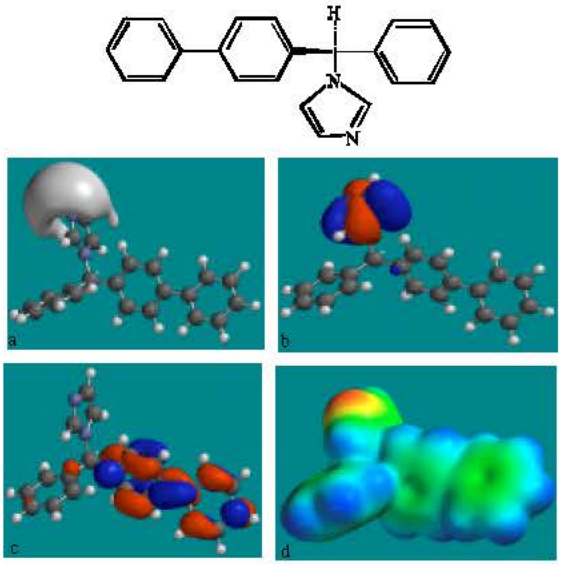

Fig. 5: Structure of R-BFZ giving in: (a) the electrostatic potential (greyish envelope denotes negative electrostatic potential), (b) the HOMOs, (where red indicates HOMOs with high electron density) (c) the LUMOs (where blue indicates LUMOs) and in (d) density of electrostatic potential on the molecular surface (where red indicates negative, blue indicates positive and green indicates neutral)

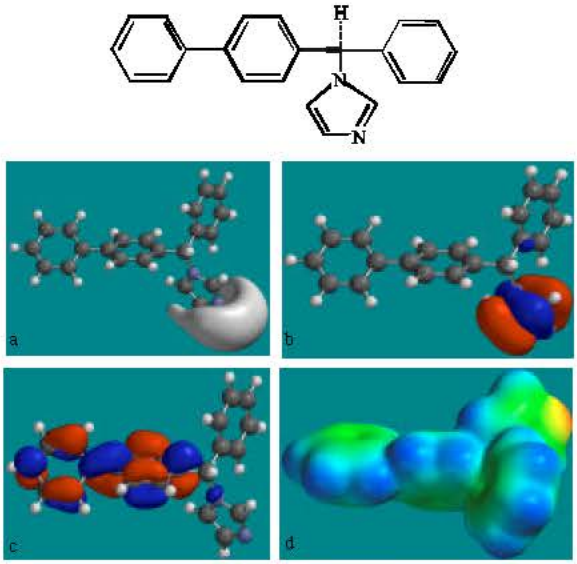

Fig. 6: Structure of S-BFZ giving in: (a) the electrostatic potential (greyish envelope denotes negative electrostatic potential), (b) the HOMOs, (where red indicates HOMOs with high electron density) (c) the LUMOs (where blue indicates LUMOs) and in (d) density of electrostatic potential on the molecular surface (where red indicates negative, blue indicates positive and green indicates neutral)

the molecular surface (where red indicates negative, blue indicates positive and green indicates neutral) in (d) as applied to optimised structures of R-LLZ, S-LLZ, R-LCZ, S-LCZ R-BFZ and S-BFZ.

The LUMO-HOMO energy differences for R-LLZ, S-LLZ, R-LCZ, S-LCZ R-BFZ and S-BFZ from DFT calculations are found to range from 4.4 to 5.0 eV, indicating that the compounds would be moderately inert kinetically.

The solvation energies of R-LLZ, S-LLZ, R-LCZ, S-LCZ R-BFZ and S-BFZ obtained from PM3 calculations are found to range from -8.5 to -10.1 kcal mol^{-1}, indicating that the compounds would be moderately soluble in water. Based on solvation energy values R-LLZ would be expected to have slightly greater solubility in water than L-LLZ.

Significantly higher dipole moment of S-LLZ than R-LLZ indicates that enantiomers can differ in dipole moment values (Table 1).

In the case of R-LLZ, S-LLZ, R-LCZ and S-LCZ, the electrostatic potential is found to be more negative around the imidazole nitrogens and acetonitrile moiety, indicating that the positions may be subject to electrophilic attack. In the case of R-BFZ and S-BFZ also, the electrostatic potential is found to be more negative around the imidazole nitrogens, indicating that the positions may be subject to electrophilic attack.

In the case of R-LLZ, S-LLZ, R-LCZ and S-LCZ, the HOMOs with high electron density are found to be less widely distributed than the LUMOs which cover essentially all the non-hydrogen atoms. In the case of R-BFZ and S-BFZ also, the HOMOs with high electron density are found to be less widely distributed than the LUMOs.

The overlap of HOMO with high electron density and region of negative electrostatic potential at some positions, gives further support to the idea that the positions may be subject to electrophilic attack.

The molecular surfaces of R-LLZ, S-LLZ, R-LCZ, S-LCZ, R-BFZ and S-BFZ are found to possess significant amounts of electron-deficient (blue) regions so that they may be subject to nucleophilic attacks such as those by glutathione and nucleobases in DNA. Reaction with glutathione can induce cellular toxicity by compromising the antioxidant status of the cell whereas that with nucleobases in DNA can cause DNA damage. However, as stated earlier, since R-LLZ, S-LLZ, R-LCZ, S-LCZ, R-BFZ and S-BFZ are all expected to be kinetically inert, the rate of such adverse reactions may be low unless speeded up enzymatically.

CONCLUSION

LLZ, LCZ and BFZ are optically active azole derivatives developed for use as antifungal agents in medicine and agriculture. Molecular modelling analyses based on molecular mechanics, semi-empirical (PM3) and DFT (at B3LYP/6-31G* level) calculations show that LLZ, LCZ and BFZ have LUMO-HOMO energy differences ranging from 4.4 to 5.0 eV indicating that the compounds would be moderately inert kinetically with BFZ being most inert. The molecular surface of R-LLZ, S-LLZ, R-LCZ, S-LCZ, R-BFZ and S-BFZ are all found to possess significant amounts of electron-deficient (blue) regions so that they may be subject to nucleophilic attacks such as those by glutathione and nucleobases in DNA. Reaction with glutathione can induce cellular toxicity by compromising the antioxidant status of the cell whereas that with nucleobases in DNA can cause DNA damage. However, because of the kinetic inertness of R-LLZ, S-LLZ, R-LCZ, S-LCZ, R-BFZ and S-BFZ, the rate of such adverse reactions are expected to be low unless speeded up enzymatically.

ACKNOWLEDGMENT

Fazlul Huq is grateful to the Discipline of Biomedical Science, School of Medical Sciences. The University of Sydney for the time release from teaching.

REFERENCES

Henry, M. and H.D. Sisler, 1984. Effects of biosynthesis-inhibiting (SBI) fungicides on cytochrome P-450 oxygenations in fungi. Prestic. Biochem. Physiol., 22: 262-275.

Koga, H., Y. Tsuji, K. Inoue, K. Kanai, T. Majima, T. Kasai, K. Uchida and H. Yamaguchi, 2006. *In vitro* antifungal activity of luliconazole against clinical isolates from patients with dermatomycoses. J. Infect. Chemother., 12: 163-165.

Niwano, Y., H. Koga, H. Kodama, K. Kanai, T. Miyazaki and H. Yamaguchi, 1999. Inhibition of sterol 14 a-demethylation of Candida albicans with NND-5-2, a novel optically active imidazole antimycotic agent. Med. Mycol., 37: 351-355.

Spartan '02, 2002. Wavefunction, Inc. Irvine, CA, USA.

Uchida, K., Y. Nishiyama and H. Yamaguchi, 2004. *In vitro* antifungal activity of luliconazole (NND-502), a novel imidazole antifungal agent. J. Infect. Chemother., 10: 216-219.